ISSN 2079-1372 Problems of Tribology, V. 31, No 3/121-2026, 36-47

Problems of Tribology
Website: http://tribology.khnu.km.ua/index.php/ProbTrib
E-mail: tribosenator@gmail.com

DOI: https://doi.org/10.31891/2079-1372-2026-121-3-36-47

Characteristics of the lubricating action of oils under EHD conditions in the local friction contact zone

O. Milanenko* 0000-0002-8197-5277, **I. Bogdanov**0000-0001-6346-4388, **D. Leusenko**0000-0001-8024-6104, **O. Vansovskyi** 0009-0000-8451-6685, **D. Stetskyi**0009-0005-2610-1947
National Transport University, Kyiv, Ukraine
**E-mail: milanmasla@gmail.com*

Received: 05 July 2026: Revised 30 July 2026: Accept: 15 August 2026

Abstract

Based on the newly developed interferometric test stand for evaluating lubricant film thickness — which enables the high-precision recording and analysis of transient processes under EHD lubrication conditions in the local friction contact zone of the non-conforming assemblies with varying actual contact geometries — across a wide range of operating (kinematic and load) parameters, an assessment was made of the influence of velocity, contact load, friction pair materials, the rheological properties of the lubricants and the geometry of the contact shape on the process of forming the minimum and central thicknesses of the lubricant film and the lubricating action of oils within the framework of determining the lubricant film parameter.

Key words: lubricating action of oils, elastohydrodynamic (EHD) lubrication, interferometric test stand, lubricant film thickness, local friction contact zone, non-conforming assemblies, contact geometries, actual contact shape, rheological properties, elliptical contact, point contact, ellipticity parameter.

An overview of unresolved issues based on the latest research and publications

Improving the lubricating performance of oils in bearing assemblies with localized contact is currently a promising and effective method for optimizing the design of rolling bearings by modifying the geometry of the contact patch and rationally selecting lubricants based on their viscosity and rheological properties. Ultimately, this leads to an increase in the service life of rolling bearing friction pairs (Fujita et al., 2019; Morales-Espejel & Félix-Quiñonez, 2021).

Theories of contact mechanics and lubrication, particularly the EHD theory, were originally based on the mechanics of continuous media, which assumes homogeneous and continuous (Newtonian) properties of lubricants regardless of scale in space and time. This approach is often valid when solving scientific and engineering problems related to surface interactions on a macroscopic scale. However, it has become clear that macroscale phenomena-such as load-carrying capacity, performance, efficiency and durability/reliability of various machines and their components-depend to a significant extent on the properties of interfaces at the macro- and microscales, where approaches that go beyond the mechanics of continuous liquid are required. Using existing EHD models, for example, it is possible to numerically simulate the entire transition from full-film (liquid) lubrication to mixed lubrication, or to boundary lubrication and surface contact, and the calculated thickness of the lubricant film can be as small as a few micrometers or even a few nanometers.

However, key questions remain unanswered, such as: Can we reliably predict interphase mechanisms using a model based on continuum mechanics if the thickness of the lubricating film is of the same order of magnitude as the oil molecules? What is the scope of application of the EHD theory? How can we model microfilms, which are commonly found under EHD and mixed lubrication conditions?

Comprehensive models and methods are currently being developed that combine continuum mechanics with the simulation of events at the micro- and even molecular levels. Recent studies include the work of Faraji et al. (2023) and Liu et al. (2020), among others. This appears to be a new and promising area of interfacial research. The mechanics of interphase regions allows for a better description of the complex nature of future studies and may be closely linked to research projects that delve into surface interactions. Today, there is a modern approach to lubrication regimes based on the consideration of two main physical aspects: elastic deformations of friction surfaces and the piezo viscosity coefficient of lubricant films (Kaneko, 2022, 2023, 2024a, 2024b, 2025). Thus, the characteristics of the EHD lubrication regime lie in the formation of high pressure in the local friction contact zone, which leads to an increase in oil viscosity and elastic deformation of the interacting friction surfaces, thereby promoting the formation of a hydrodynamic lubricating film. This lubrication regime is predominantly observed in non-conformal friction assemblies (bearing assemblies) with a localized contact configuration. Under heavy loads, the pressure generated in the contact zone reaches 1 GPa. Since the lubrication regime is a complex phenomenon, there is a need to improve experimental methods for measuring lubricant film thickness and to conduct a comparative evaluation of calculated and experimental data on lubricant film thickness during the development of a mathematical model.

Problem Statement

The analysis of the characteristics of EHD lubrication discussed above showed that this operating regime is typical of non-conformal contact lubrication, which ensures minimal friction and a long service life for machine components. This occurs due to the formation of a continuous lubricating film, which prevents direct contact between the micro-irregularities of the contacting friction surfaces, as determined by the lubricating film parameter λ according to the following expression:

$$\lambda = \frac{h_{min}}{\sqrt{R_{a1}^2 + R_{a2}^2}}, \tag{1}$$

where h_{min} – minimum thickness of the lubricating film in the local contact zone for EHD friction conditions;

$\sqrt{R_{a1}^2 + R_{a2}^2}$ – the arithmetic mean deviation of the roughness profile from the centerline for each surface of a friction pair.

In this regime, the lubricating action of oils in the local contact zone will depend on the geometry of the actual contact shape and the rheological and viscosity properties of the lubricant film, since the pressure increases significantly under load, especially in the zone at the exit from the contact. Therefore, considering the geometry of the contact shape by evaluating the ellipticity coefficient and selecting the elastic-piezo viscous regime by evaluating the piezo viscosity coefficient will allow for a more accurate assessment of the lubricant film thickness under real operating conditions for bearing friction assemblies.

Thus, solving the multifactorial problem of estimating the lubricant film thickness under EHD lubrication conditions for non-conforming (bearing) friction assemblies requires the use of modern automated equipment capable of evaluating the transient processes occurring in the lubricant film within the actual local friction contact zone. Experimental methods for measuring the thickness of the lubricant film in the EHD lubrication systems in the local contact zone can be divided into the following groups: electrical, X-ray, acoustic, and optical methods.

Currently, optical measurement methods are the most accurate and visually representative methods for studying lubricant film thickness under EHD lubrication conditions for local friction contacts (Kazuyuki et al., 2021; Šperka et al., 2016). These methods allow for real-time measurement of film thickness with nanometer-level accuracy. Among them, the optical interference method is exceptionally effective, as it allows for measuring film thickness with an accuracy of 0.05 μm or less. The difference between theoretical and experimental film thickness values typically does not exceed 1%.

Four optical interference methods can be identified that are optimally suited for estimating the thickness of the lubricating film under EHD lubrication conditions: the traditional optical interference method, the spatial layer imaging method (SLIM), thin-film colorimetric interferometry and the method for determining the relative intensity of optical interference.

The traditional optical interference method reveals the complete relative topographical distribution of the contact area. Typically, this technique is used to measure film thicknesses of 0.05 μm and greater, with a 1% difference between theoretical and experimental values for the SAE 40 medium-viscosity oil.

The Spatial Layer Imaging Method (SLIM) measures lubricant film thickness at the nanoscale by incorporating a solid interlayer (Wolf et al., 2022) with a refractive index like that of the oil. The thickness of the intermediate layer is subtracted from the total thickness (oil and intermediate layer) to measure film thickness down to 10 nm. The difference between the theoretical and experimental values for the minimum and central film thicknesses at low shear rates is approximately 30% and 25%, respectively. In thin-film colorimetric interferometry, computer software is used for comprehensive image processing, which allows for the real-time determination of the film thickness distribution using colorimetric interferometry. The measurement range for this method is from 1 to 800 nm, with a resolution of 1 nm and a spatial resolution of 1 μm. The presence of the EHD film with a thickness on the order of several tens of molecular dimensions has been confirmed using this method.

The method for determining the relative intensity of optical interference uses monochromatic light, which produces Newton’s interference rings. To measure the thickness of the lubricating film at a specific location, the relative intensity of light at the locations of the maximum and minimum Newton’s rings is examined by analyzing a digitized image, where it was found that the thickness of the lubricating film is approximately 1 nm (Khan et al., 2021). This method was refined by Khan et al. (2021) for measuring film thickness, but it has certain limitations. For example, in the case of point (circular) contact, the film takes on a horseshoe shape, and the point of minimum film thickness is located on one of the sides distant from the centerline due to the use of a reflective sphere and a transparent disk with a high-precision coating.

The above considerations regarding experimental studies of the lubricating action of oils indicate that optical methods are widely used for measuring film thickness, as they allow for the measurement of lubricant layer thickness down to 1 nm or even less. However, according to the specified task, the complete test setup must have the following characteristics:

1) Visual observation of changes in the geometry of the actual contact shape, from point (circular) to elliptical contact with a wide range of ellipticity;

2) Color chromatic and filtered illumination of the entire local friction contact zone.

3) Computer software for comprehensive image processing and automated control of the operating characteristics of friction pairs, like the results obtained using thin-film colorimetric interferometry.

4) Stroboscopic illumination for photo and video recording of the interference pattern to evaluate transient processes occurring in the thin-film lubricant layer.

Thus, taking into account the specific nature of the research described above in accordance with the stated task, it is necessary to develop test equipment that implements the traditional method of optical interference using software for comprehensive image processing and automated control of the operating characteristics of friction pairs, as is characteristic of thin-film colorimetric interferometry.

Methodological tools for evaluating the lubricating performance of oils under EHD lubrication conditions in the local friction contact zone

The necessary information regarding the nature of many phenomena in local friction contact zones can be obtained only by applying a fundamentally new and modern approach to enhancing the lubricating performance of oils for specific operating conditions and lubrication regimes, as well as predicting the service life of friction assemblies for the range of lubricants under study. This is achieved by selecting an effective conceptual framework for conducting experimental research, utilizing the necessary modern and automated equipment, applying modern methods of mathematical analysis of research results, and implementing the findings of experimental studies at lubricant manufacturers or operators of friction assemblies.

To implement the above concept and taking into account the necessary requirements for testing equipment, an interference testing stand was developed based on the method of optical light interference, which allows for the assessment of the lubricant film thickness and lubrication regime in the local and elastic zones of the actual contact area, as well as beyond its boundaries at the entry and exit points of the contact, taking into account changes in the geometry of the contact shape due to the ellipticity coefficient and the viscous and rheological properties of the tested series of lubricants. The use of photo and video equipment makes it possible to record and analyze, with high precision, the transient processes under EHD lubrication conditions that occur in the micro zones of local friction contact in ball and barrel-shaped roller bearings, ball friction gears, ball bearings with an external self-aligning support and slewing ring over a wide range of operating (kinematic and load) parameters.

A general view of the test stand is shown in Fig. 1.

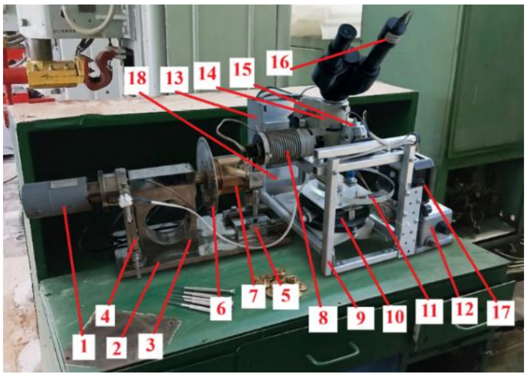

1 – D-38T electric motor; 2 – base plate; 3 – frame; 4 – centering device;
5 – carriage assembly with freely moving supports for the “glass outer ring (indenter 1) – steel ball (counterbody)” friction pair; 6 – perforated disc for determining rotational speed (linear velocity); 7 – glass outer ring (indenter 1);
8 – lighting unit; 9 – frame; 10 – specimen stage with a carriage featuring freely moving supports, assembled for the friction pair “glass disc (indenter 2) – steel ball (counterbody)”; 11 – glass outer disc (indenter 2);
12 – illumination lamp ignition unit; 13 – power supply unit; 14 – MMU-3 microscope; 15 – RS775 electric motor;
16 – camera; 17 – primary data processing unit (load, rotational speed, and temperature);
18 – power supply unit for the RS775 and D-38T electric motors

Fig. 1. Test setup for interference studies of lubricant film thickness, considering changes in the geometry of the actual local friction contact shape

The object of study (Fig. 2a, b) is the contact zone between an outer glass ring (see Fig. 2a) serving as indenter 1 or a glass disc (see Fig. 2b) serving as indenter 2, both made of the K7 optical glass with a surface finish of Ra1 = 0.02 μm (roughness class – 12b) and a standard steel ball serving as the counterbody, made of SHKH-15 steel with a surface finish of Ra2 = 0.1 μm (roughness class – 10b); the ball’s diameter is 25.4 mm.

Thus, the arithmetic mean deviation of the roughness profile from the mean line of the friction pairs, $\sqrt{R_{a1}^2 + R_{a2}^2}$, will be 0.102 μm for determining the lubrication mode parameter λ using equation (1). The K7 optical glass, from which indenters 1 and 2 are made (see Fig. 2a, b), is a type of colorless crown optical glass (crown class) characterized by a refractive index of approximately n_d = 1.511. It belongs to the classic light crown glasses and is used for manufacturing lenses and other components of optical instruments.

The design of the carriage with freely moving supports (see Fig. 2a, b) allows the counterbody to be repositioned relative to the corresponding indenters 1 and 2 to change the geometry of the friction contact shape (the ellipticity coefficient k). Thus, this configuration enables rolling friction conditions for the "steel ball–glass ring" friction pair to simulate the operating conditions of ball and barrel-shaped roller bearings and ball friction gears, as well as for the "steel ball – glass disc" friction pair to simulate the operating conditions of ball bearings with an external self-aligning support and swivel ring (plate). Ball carriages with freely moving supports 2 (see Fig. 2a) for elliptical contacts and 3 (see Fig. 2b) for point contacts consist of a metal housing, two freely moving shafts onto which four small MR-series ball bearings (supports) measuring 4x8x3 mm are pressed to accommodate the ball as a counterbody, and the Type K thermocouple to determine the bulk temperature of oil.

To experimentally measure the optical thickness of the lubricating film, an MMU-3 microscope was used, as shown in the diagram (Fig. 3). This microscope is designed for examining opaque objects in reflected light and is used for both bright-field and dark-field observation under polarized light.

a

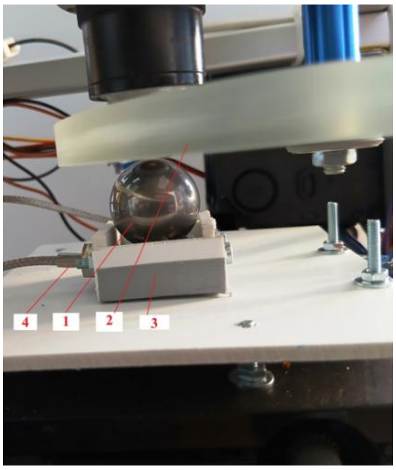

b

a – "Glass outer ring (indenter 1) – steel ball (counterbody)" friction pair: 1 – glass outer ring (indenter 1); 2 – carriage with freely moving supports; 3 – thermocouple; 4 – steel ball (counterbody)
b – "Glass disk (indenter 2) – steel ball (counterbody)" friction pair: 1 – steel ball (counterbody); 2 – glass disk (indenter 2); 3 – carriage with freely moving supports; 4 – thermocouple

Fig. 2 a, b. Friction pairs of the test rig for interference studies of lubricant film thickness as the geometry of the actual local friction contact shape changes

To avoid having to reposition the microscope 14 (see Fig. 1), the following procedure was followed: the stand on which the microscope is mounted was raised an additional 200 mm from its baseline position using a special screw. This compensates for the difference in height between the disk and the ring. Additionally, the microscope can rotate 360° on the stand. If the upper power supply unit 13 (see Fig. 1) is in the way, it can be removed; the length of the wires allows for this. When performing point-contact experiments, the microscope is rotated 90° from its initial position (see Fig. 1). The high-speed camera 16 (see Fig. 1), mounted on the microscope, is used to transmit the image from the microscope's eyepieces to PC.

Power supplies 18 for motors (see Fig. 1) are connected to 230 V, 50 Hz power supply and feature switch buttons 15 for motor (RS775), a powerful brushed DC motor, and motor 1 (D-38T), an aviation DC motor. Power supply unit 13 (see Fig. 1), rated for 12 V, 5 V and 3.3 V, respectively, powers the rest of the system's electrical components: the lighting lamp ignition unit 12 and the primary data processing unit 17 (see Fig. 1).

The lighting lamp ignition unit 12 (see Fig. 1) features a dimmer for smoothly adjusting light brightness and saving electricity and provides an uninterrupted power supply to the lighting lamp unit 8 (see Figs. 1 and 3).

The primary data processing unit 17 (see Fig. 1) consists of:

– the type K thermocouple with a digital amplifier based on the MAX6675 integrated circuit (see Figs. 2a, b);

– the flat "Kvasolina"-type strain gauge for the low platform based on the HX711 (Fig. 4);

– the compact HW-201 infrared obstacle sensor based on reflected light, with adjustable range and a supply voltage from 3.3 to 5 V, which is also used in robotics for obstacle avoidance and in simple control systems (see Fig. 4);

– the compact and popular Arduino Nano V3.0 development board based on the ATmega328P microcontroller, which operates at 16 MHz at 5 V and can be easily mounted on a breadboard (see Fig. 4).

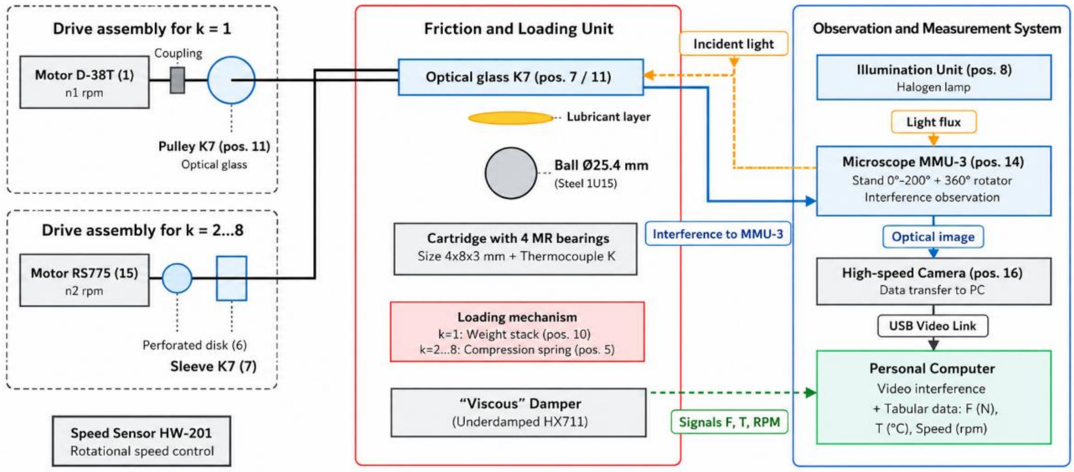

Fig. 3. Schematic kinematic and optical diagram of a test rig for interference studies of lubricant film thickness, considering changes in the geometry of the actual local friction contact shape

The initial results are transmitted to PC, where the input parameters are processed (see Figs. 3 and 4). The software used includes Windows 11 Pro 25H2 x64, the built-in "Camera" app, and Arduino IDE 2.3.5 to automate the measurement equipment.

To determine the rotational speed, a perforated disk for elliptical contacts 6 (see Fig. 1) with the ellipticity coefficient k > 1 (see Fig. 2a) and markings on a glass disk 11 (see Fig. 1) for point contacts for k = 1 (see Fig. 2b).

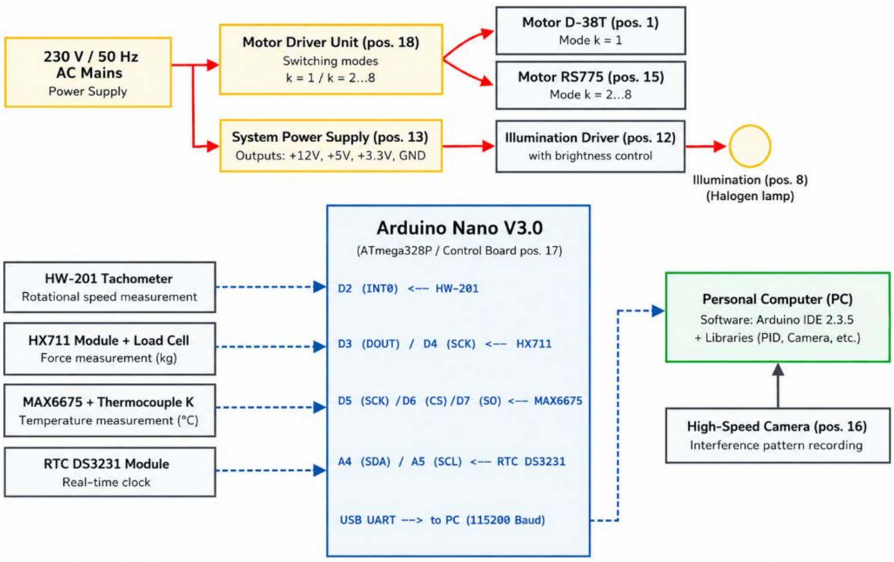

Fig. 4. Schematic electrical diagram of a test bench for interference studies of lubricant film thickness, considering changes in the geometry of the actual local friction contact

The HW-201 infrared obstacle sensor (see Figs. 3 and 4), which is part of the primary data processing unit 17 (see Fig. 1), is repositioned and mounted in a special hole in the base 3 or frame 9, depending on which contact shape is being tested: elliptical (base) or point (frame). The base 3 is mounted on a special plate 2 and has a centering device 4, which centers the entire "glass outer ring (indenter 1) – steel ball (counterbody)" friction pair system.

To study elliptical contacts, where k > 1, the "glass outer ring (indenter 1) – steel ball (counterbody)" friction pair is used (see Fig. 2a), in which the load is applied via a carriage and a lever system 5 (see Fig. 1). To study point contacts, where k = 1, a friction pair consisting of a "glass disk (indenter 2) – steel ball (counterbody)" is used, in which the load is applied via a specimen stage with a carriage assembly 10 (see Fig. 2b), which allows the stage to be moved within certain limits in the x and y directions, as well as rotated 360°. A membrane is mounted on the stage, on which the carriage is positioned and beneath which the "Kvasolina"-type load cell for the low platform on the HX711 is located (see Figs. 3 and 4).

The actual shapes (micro-interferograms) of elliptical and point contacts under dynamic friction conditions, shown in Fig. 5a, b, respectively, were obtained using the optical interference method on an interference testing bench.

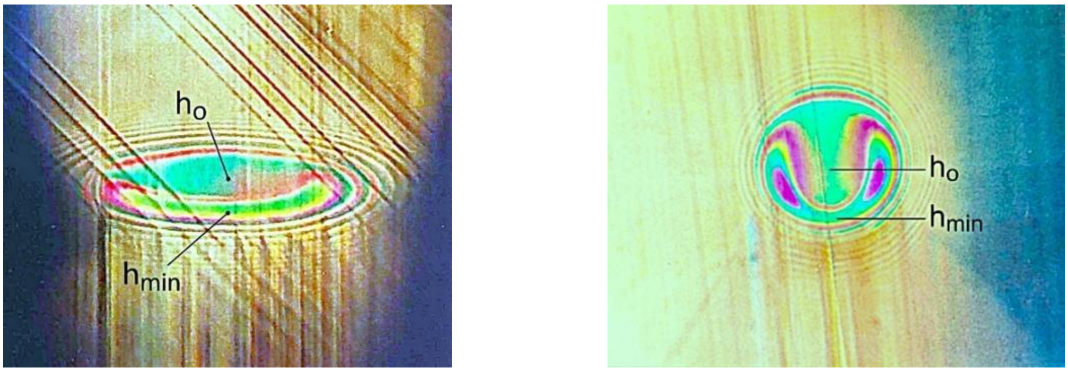

a b

h_{min} – minimum lubricant film thickness; h_o – central lubricant film thickness

Fig. 5 a, b. Actual shapes (micro-interferograms) of elliptical (a) and point (b) contacts under dynamic friction conditions

Fig. 5a, b shows all the characteristic features of lubrication under varying contact geometry, as observed on the developed interferometric test bench. The elliptical and point contact shapes (see Fig. 5a, b) have corresponding lubricant film thickness distributions with minimum thickness values at the contact exit (hmin) and in the central contact region (ho), which arise between the contact surfaces of friction bearing assemblies.

Results of the assessment of the influence of key parameters on lubricant film thickness

The most important practical aspect of lubrication analysis for local friction contact is determining the minimum (h_{min}) and central (h_o) lubricant film thicknesses in the local friction contact zone, since maintaining the required lubricant film thickness is crucial for the operational reliability of various friction bearing assemblies. The influence of the contact geometry—expressed in terms of ellipticity—and the dimensionless parameters of velocity, load, and materials on the corresponding lubricant film thicknesses and parameters is investigated for a local contact that is fully immersed in the lubricant (i.e., for a heavily lubricated contact).

Changes in the main input and dimensionless parameters used for the experimental studies are presented in Table 1.

The input and dimensionless parameters for the implementation of the EHD lubrication regime, as shown in Table 1 and considering changes in ellipticity in a point friction contact, do not cover all real-world lubrication conditions for local friction contacts. From a practical standpoint, it is important to estimate the thickness of the lubricant film, taking into account the influence of changes in the geometry of the contact shape—that is, its ellipticity—the rheology of lubricants, and the wear of the friction pair surfaces due to roughness, in order to achieve an optimal lubrication regime that enhances the lubricating effect of the oils.

1. Assessment of the effect of lubricant film thickness on rolling velocity

By varying one of the parameters, it is possible to determine the optimal lubricant film thickness that affects the lubricating performance of oils in the local contact zone of rolling bearings when using transmission oils for various technical applications.

The range of linear rolling velocity V varied from 0.05 to 1.0 m/s; the oil temperature T remained at 343 K throughout the experiment; the maximum contact pressure P_{max} = 474 MPa. The minimum thickness h_{min} and the thickness of the lubricant film in the central contact zone h_o were measured using the optical interference method on an interference testing stand for EHD point-contact (R_y/R_x = 1) based on a sample of micro-interferograms (Fig. 6).

A graphical interpretation of the experimental results showing the effect of rolling velocity V on the minimum lubricant film thickness h_{min} and the central lubricant film thickness h_o in the point contact zone (R_y/R_x = 1) for the entire range of oils studied is presented in Fig. 7a, b, respectively.

Fig. 7c shows the dependence of the lubricant film parameter λ on rolling velocity V, which demonstrates the need to ensure EHD friction conditions whilst maintaining linear rolling velocity V within the range of 0.1 to 0.5 m/s for ATF-III and SAE 75W-80 transmission oils, SAE 75W-90 and within the range of 0.05 to 0.2 m/s for SAE 80W-90 transmission oil.

Table 1

Key input and dimensionless parameters for the implementation of the EHD lubrication regime for local friction contact

№	Parameter	Symbol	Formula	Measurement range	Dimension
1) Geometric parameters of the local friction contact					
1	Ratio of Curvature Radii	R_y/R_x	-	1 - 25	-
2	Relative radius of curvature along the direction of rolling	R_x	-	0,01	m
3	Contact ellipticity	k	$k = \left[{R_y}/{R_x}\right]^n$	1 – 8	-
2) Friction pair parameters					
4	The modulus of elasticity	E'	$E' = \dfrac{2}{\left(\dfrac{1-\nu_1^2}{E_1} + \dfrac{1-\nu_2^2}{E_2}\right)}$	150 - 250	GPa
3) Specifications for lubricants (transmission oils)					
5	Dynamic viscosity at 20°C	η_o	-	0,15 – 0,5	Pa·s (cP)
6	Kinematic viscosity at 100°C	μ	-	6,4 – 24,0	mm²/s (cSt)
7	Piezo-viscosity coefficient	α	$\alpha \cdot P = A \cdot \left[\left(\frac{T-138}{T_0-138}\right)^{-S_0} \cdot B^Z - 1\right]$	$(1{,}4 – 1{,}6)\cdot 10^{-8}$	Pa^{-1}
4) Operating parameters					
8	Linear rolling velocity	V	-	0,05 – 1,0	m/s
9	Contact load	F	-	5 – 50	H
10	Maximum pressure in the contact zone	P_{max}	-	600	MPa
11	Volume temperature in the oil bath	T	-	293 - 343	K
5) Measured lubricant film thicknesses and the calculated lubricant film parameter					
12	Minimum lubricant film thickness	h_{min}	-	0,08 (min)	μm
13	Central lubricant film thickness	h_o	-	1,77 (max)	μm
14	Lubricant film parameter within the range of contact ellipticity variation	λ	$\lambda = \dfrac{h_{min}}{\sqrt{R_{a1}^2 + R_{a2}^2}}$	2 - 4	-
6) Dimensionless parameters in the local EHD zone of friction contact					
15	Dimensionless velocity parameter	U	$U = \dfrac{\eta_o \cdot V}{E' \cdot R_x}$	$6{,}3\cdot10^{-12}$ – $4{,}2\cdot10^{-10}$	-
16	Dimensionless load parameter	W	$W = \dfrac{F}{E' \cdot R_x^2}$	$6{,}5\cdot10^{-7}$ – $4{,}0\cdot10^{-6}$	-
17	Dimensionless material parameter	G	$G = \alpha \cdot E'$	1500 - 4000	-
18	Dimensionless minimum lubricant film thickness	H_{min}	$H_{min} = \dfrac{h_{min}}{R_x}$	$0{,}8\cdot10^{-5}$ (min)	-
19	Dimensionless central lubricant film thickness	H_o	$H_0 = \dfrac{h_0}{R_x}$	$1{,}8\cdot10^{-4}$ (max)	-

Fig. 6. Selection of micro-interferograms for point EHD contact ($R_y/R_x = 1$) over a range of linear rolling velocity V from 0.05 to 1.0 m/s (SAE 80W-90 transmission oil)

The presented selection of micro-interferograms (see Fig. 6) and the graphical interpretation of the dependence of the minimum and central thicknesses in the EHD contact zone on the rolling velocity (see Fig. 7a,

b) quite clearly indicate the dominant influence of the rolling speed under EHD lubrication conditions. Moreover, the SAE 80W-90 transmission oil, which has the highest viscosity grade, is characterized by greater sensitivity to high- velocity (high-RPM) operating conditions of rolling bearings.

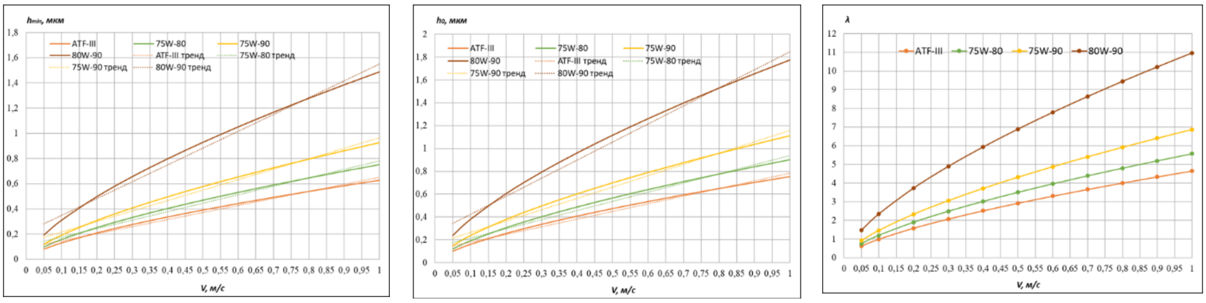

a b c

Fig. 7 a–c. Dependence of the minimum lubricant film thickness h_{min} (a), the central lubricant film thickness h_o (b) and the lubricant film parameter λ (c) in the point contact zone on the rolling velocity V

2. Assessment of the effect of contact load on the thickness of the lubricating film

By increasing the contact load from 7.78 to 46.68 N, corresponding to maximum contact pressures P_{max} ranging from 330 MPa to 600 MPa, at an oil temperature T of 343 K, the minimum and central thicknesses of the lubricant film in the point contact zone were determined on an interference measurement bench using a sample of micro-interferograms at $R_y/R_x = 1$ (Fig. 8).

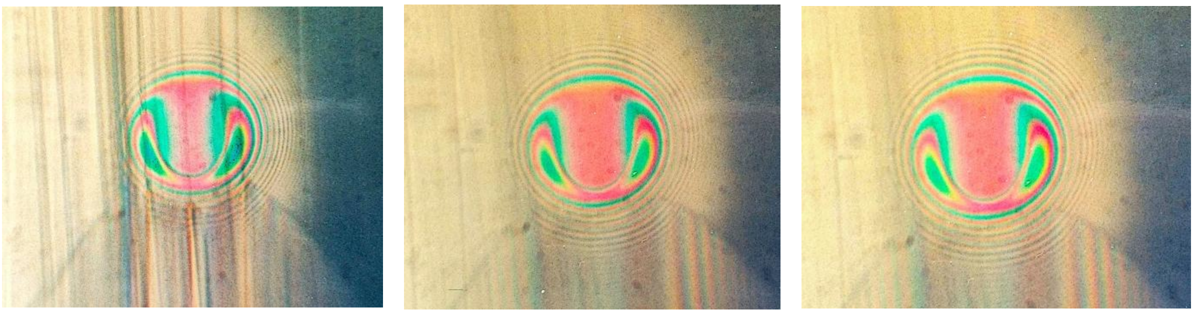

Fig. 8. Selection of micro-interferograms for a point EHD contact ($R_y/R_x = 1$) across a range of contact loads F from 7.78 to 46.68 N (the SAE 75W-90 transmission oil)

A graphical interpretation of the experimental results showing the effect of load F on the minimum lubricant film thickness h_{min} and the central lubricant film thickness h_o in the point contact zone ($R_y/R_x = 1$) for the entire range of oils studied is presented in Fig. 9a, b, respectively. Fig. 9c shows the dependence of the lubricant film parameter λ on the contact load F, which demonstrates the need to ensure the EHD friction conditions whilst maintaining the proposed contact load values F within the range of 7.78 to 46.68 N for all the transmission oils under investigation.

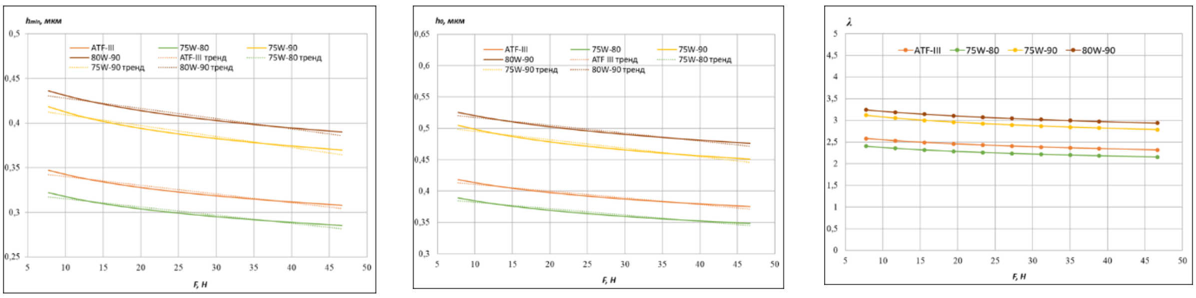

a b c

Fig. 9 a–c. Dependence of the minimum lubricant film thickness h_{min} (a), the central lubricant film thickness h_o (b) and the lubricant film parameter λ (c) in the point contact zone on the contact load F

The sample micro-interferograms presented (see Fig. 8) and the graphical interpretation of the relationship between the minimum and central thicknesses of the lubricant film in the EHD contact zone as a function of contact load (see Figs. 8 and 9a, b), clearly indicate that the load has a negligible effect on the respective thicknesses, which do not decrease significantly, as can also be seen from the color. Furthermore, as the contact load increases, the zone of central thickness expands in the transverse direction, whilst the minimum thickness at the exit from contact moves progressively further away from the central axis of the point of friction contact; this is, in our opinion, associated with the rheological effect of the oil's compressibility.

3. Assessment of the influence of materials on the lubricant film thickness

Unlike the determination of the influence of rolling velocity V and contact load F on the respective thicknesses under investigation, the influence of materials cannot be determined by simply changing just one parameter, since the dimensionless material parameter G comprises two variables (see Table 1), one of which characterizes the properties of the friction pair surfaces – the reduced modulus of elasticity E' – and the other – the rheological properties of the lubricant via the piezo-viscosity coefficient α. Therefore, four groups of materials, *G1–G4*, were formed, comprising three friction pairs made of different materials when using the range of lubricating oils under investigation, which have different viscosity classes and operational purposes and are used for the lubrication of modern rolling bearing assemblies. Three friction pairs, which are used in many rolling bearings for automotive and agricultural applications, were used as the friction pairs under investigation; their properties are given in Table 2.

Table 2

Input parameters for friction pair materials

№	Name of the friction pair	Modulus of elasticity E_1, GPa	Modulus of elasticity E_2, GPa	Poisson's ratio ν_1	Poisson's ratio ν_2	The reduced modulus of elasticity E', GPa
1	St40KH – SHKH15	210	220	0,25	0,3	235
2	BrO10F1 – SHKH15	120	220	0,33	0,3	170
3	BrOCS-4-4-17 – SHKH15	99	220	0,37	0,3	160

Experimental studies involving four groups of materials were conducted at an average rolling velocity of V = 0.4 m/s under EHD friction conditions, with an average contact load of F = 30 N; a temperature of T = 343 K, where the minimum thickness and the central thickness of the lubricant film in the point contact were determined on an interference measurement bench based on a sample of micro-interferograms at $R_y/R_x = 1$.

The experimental results showing the effect of material groups *G1–G4* on the minimum thickness h_{min} and the central thickness h_o of the lubricant film at $R_y/R_x = 1$ for the entire spectrum of oils studied are presented as a graphical interpretation of the data in Fig. 10a, b, respectively, for the four oils studied.

Based on the results of experimental studies of the effect of the material parameter G on the minimum thickness h_{min} and the central thickness h_o of the lubricating films in the point contact zone, a negligible effect—up to 3%—was found, specifically of the friction pair materials based on the reduced modulus of elasticity E', as indicated by the slight slope of the linear dependencies relative to the x-axis with respect to the dimensionless material parameter G. It is precisely the piezo-viscosity coefficient α that has a significant influence on the formation of film thicknesses under EHD conditions, as confirmed by the significant divergence of the dependencies for four transmission oils differing in viscosity class and intended use. If we take the material data for the groups (see Table 2) for the St40KH – SHKH15 friction pair, which experiences a maximum pressure P_{max} = 474 MPa in the point EHD contact zone, we obtain the following: for ATF II transmission oil, $\alpha \approx 0.014$ MPa^{-1}, and the dynamic viscosity η will increase by a factor of 762; for SAE 75W-80 transmission oil, $\alpha \approx 0.015$ MPa^{-1}, and the dynamic viscosity η will increase by a factor of 1 224; for SAE 80W-90 transmission oil — $\alpha \approx 0.016$ MPa^{-1}, and the dynamic viscosity η will increase by a factor of 1 970. In other words, the dynamic viscosity η of the high-viscosity SAE 80W-90 transmission oil increases by nearly three times compared to that of the low-viscosity ATF III transmission oil, which underscores the importance of the rheological properties of lubricants.

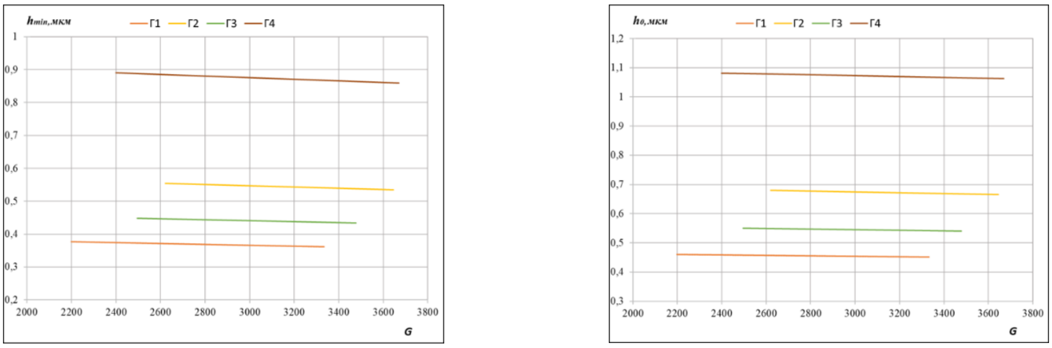

a b

Fig. 10a, b. Effect of the dimensionless material parameter G on the minimum thickness h_{min} (a) and the central thickness h_o (b) lubricant films in the point contact zone for different of material groups G1–G4

From the perspective of the influence of materials G on the lubricant film parameter λ, this is not correct, since this parameter determines the lubrication regime, rather than the quality characteristics of the materials, which specifically affect the strength of the lubricant films and the durability of the friction pairs.

4. Assessment of the patterns of how contact ellipticity affects lubricant film thickness

One of the least studied aspects of the EHD theory of point contact lubrication is the effect of changes in contact geometry due to an increase in its ellipticity k. The ellipticity k depends on the dimensions of the contact ellipse in the Y and X directions (the rolling direction) and on the ratio of the relative radii of curvature R_y/R_x of the friction pair, ranging from unity for a disk–ball pair to approximately eight when the contact geometry is close to linear contact.

Thus, by varying the ratio of curvature radii R_y/R_x of the friction pair, while keeping the rolling velocity V, contact load F, and material groups *G1–G4* constant to ensure the friction conditions specified in Table 1, the minimum and central thicknesses of the lubricant film in the point-contact zone were determined on an interference measurement bench based on a sample of micro-interferograms at $R_y/R_x = 1$ (Fig. 11a) and at $R_y/R_x = 8$ (Fig. 11b) when maximum rolling velocities were reached.

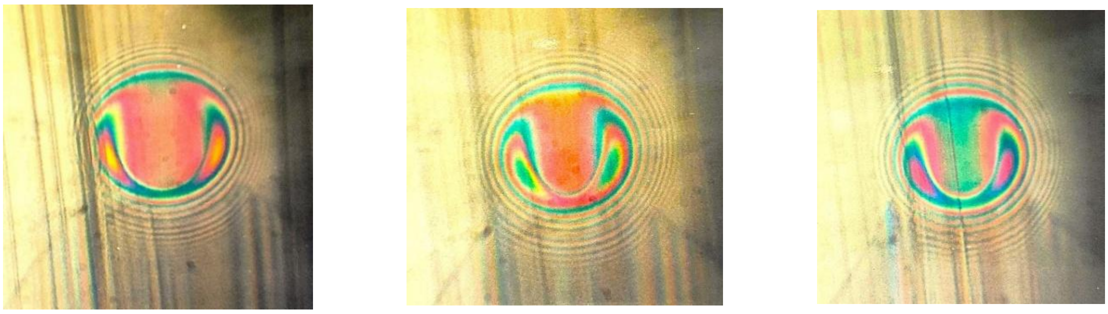

a

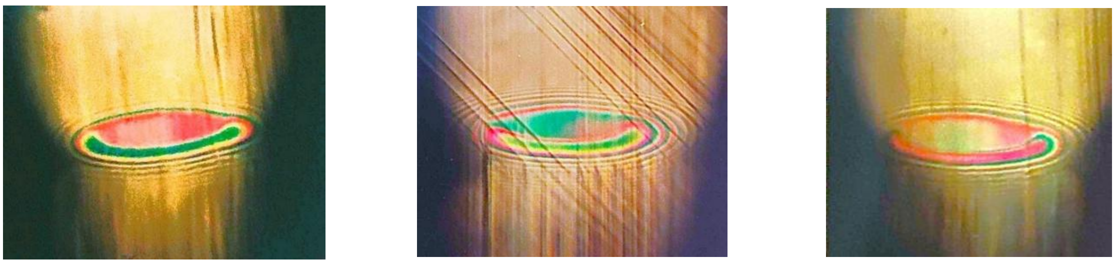

b

Fig. 11 a, b. Selection of micro-interferograms in the point EHD contact zone at $R_y/R_x = 1$ (a) and at $R_y/R_x = 8$ (b), while keeping the rolling velocity, contact load and material groups constant

At first glance, based on a sample of micro-interferograms (see Fig. 11a, b), it can be seen from the color that, while keeping the rolling velocity V, contact load F and material groups *G1–G4* remain constant, the minimum and central thicknesses of the lubricant film in the friction contact zone remain virtually unchanged as the contact ellipticity increases due to a change in the ratio of curvature radii from $R_y/R_x = 1$ *(a)* to $R_y/R_x = 8$ *(b)*. However, if we look closely at the micro-interferograms taken at the maximum rolling velocity (see Fig. 11a, b) and compare the minimum thicknesses at the exit from the contact zone, we see that when maximum rolling velocities are reached, the minimum thickness at the exit from the contact zone for the elliptical EHD contact ($R_y/R_x = 8$) will be slightly higher than that for the EHD point contact ($R_y/R_x = 1$). This effect is explained by the fact that as the ellipticity of the contact shape increases, the peak pressure decreases, which leads to a slight increase in the minimum thickness at the exit from the contact — this parameter that is more sensitive to changes in the contact geometry. The observed effect of reduced peak pressure can be a very important aspect of optimizing the design of friction bearing assemblies.

Experimental results showing the effect of contact ellipticity k on the minimum thickness h_{min} and the central thickness h_o of the lubricant film across the entire range of the curvature radius ratio R_y/R_x —from point-contact ($R_y/R_x = 1$) to practically linear ($R_y/R_x = 25$) contact, for the entire spectrum of oils studied, are presented in graphical form in Fig. 12a, b for the four oils under investigation.

Fig. 12c shows the dependence of the lubricant film parameter λ on the contact ellipticity k, with regard to ensuring the EHD friction conditions, where it is necessary to adhere to the proposed values of contact ellipticity ranging from 1 to 8 and the curvature radius ratio R_y/R_x ranging from point ($R_y/R_x = 1$) to practically linear ($R_y/R_x = 25$) contact for all the transmission oils under study.

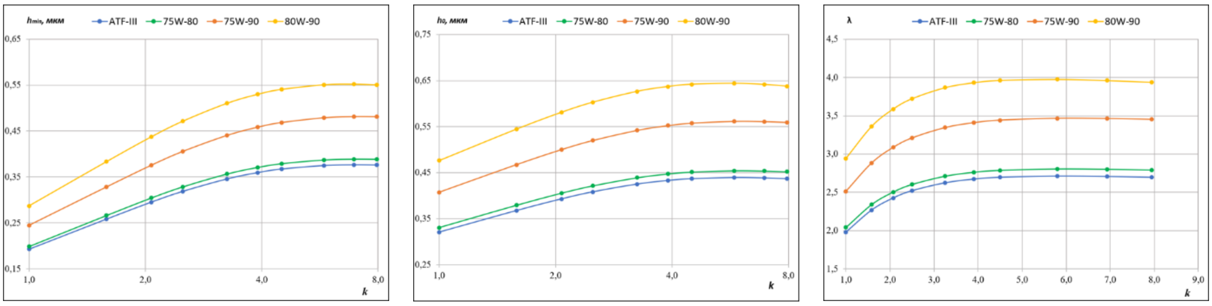

a b c

Fig. 12 a–c. Dependence of the minimum lubricant film thickness h_{min} (a), the central lubricant film thickness h_o (b) and the lubricant film parameter λ (c) on the contact ellipticity k across the entire range of the curvature radius ratio R_y/R_x

Conclusions

1. The dominant influence of rolling velocity under EHD lubrication conditions on the formation of the lubricant film thickness was established, with the dimensionless rolling velocity parameter varying by nearly two orders of magnitude when using four transmission oils differing in viscosity class and rheological properties. Furthermore, it was determined that transmission oils with a high viscosity class are characterized by greater sensitivity to high-speed (high-RPM) operating conditions of rolling bearings.

2. As the contact load increases by nearly one order of magnitude of the dimensionless load parameter when using four transmission oils differing in viscosity class and rheological properties, the manifestation of oil compressibility was observed, which is associated with the expansion of the central thickness zone in the transverse direction and the minimum thickness at the exit from contact becomes increasingly distant from the central axis of the point contact, which confirms the importance of taking into account the rheological properties of the studied series of transmission oils.

3. Using four groups of materials—comprising three pairs of friction materials and four transmission oils differing in viscosity class and rheological properties — we demonstrated a significant influence of the piezo-viscosity coefficient on the lubricant film thickness, as confirmed by the substantial divergence in the dependencies for the four transmission oils studied, in contrast to the negligible influence (up to 3%) of the friction pair materials.

4. It was established that transmission oils differing in viscosity class and rheological properties respond differently to the actual pressure exerted by the lubricating film formed within the point contact friction zone; for example, it was determined that the dynamic viscosity of a high- viscous SAE 80W-90 transmission oil compared to low-viscosity ATF III transmission oil under all other operating conditions being equal.

5. The effect of reduced peak pressure has been observed upon reaching maximum rolling velocities, when the minimum thickness at the exit from contact for an elliptical EHD contact exhibits a relative increase in thickness; that is, it is more sensitive to changes in contact geometry than for a point EHD contact.

References

1. Faraji, M., Seitz, A., Meier, C., & Wall, W. A. (2023). A mortar finite element formulation for large deformation lubricated contact problems with smooth transition between mixed, elasto-hydrodynamic and full hydrodynamic lubrication. *Tribology Letters*, *71*(1), Article 11. https://doi.org/10.1007/s11249-022-01682-4

2. Fujita, T., Hasegawa, N., Kamura, N., & Sasaki, T. (2019). Rolling contact fatigue of thrust ball bearing under low lambda condition. *Tribology Online*, *14*(4), 163–172. https://doi.org/10.2474/trol.14.163

3. Kaneko, M. (2022). High pressure rheology of lubricants (Part 5) - Derivation of van der Waals type viscosity equation. *Tribology Online*, *17*(4), 257–275. https://doi.org/10.2474/trol.17.257

4. Kaneko, M. (2023). High pressure rheology of lubricants (Part 1) - Deriving equation of relations of pressure, temperature, density and the viscosity. *Tribology Online*, *18*(4), 136–149. https://doi.org/10.2474/trol.18.136

5. Kaneko, M. (2024a). High pressure rheology of lubricants (Part 2) - Deriving equation of relations of pressure, temperature and the density. *Tribology Online*, *19*(1), 136–149. https://doi.org/10.2474/trol.19.33

6. Kaneko, M. (2024b). High pressure rheology of lubricants (Part 7) - Derivation of van der Waals type line density equation and estimation of high pressure density. *Tribology Online*, *19*(1), 87–94. https://doi.org/10.2474/trol.19.87

7. Kaneko, M. (2025). High pressure rheology of lubricants (Part 6) - Derivation of pressure temperature linear equation of dimensionless density and estimation of high pressure density. *Tribology Online*, *20*(1), 36–45. https://doi.org/10.2474/trol.20.36

8. Kazuyuki, Y., Kazuyuki, N., & Joichi, S. (2021). Influence of the heat transfer field on anomalous lubricant film formation in elastohydrodynamic lubrication conditions. *Tribology Letters*, *114*, Article 114. https://doi.org/10.1177/1350650121997240

9. Khan, T., Tamura, Y., Yamamoto, H., Morina, A., & Neville, A. (2021). Investigation of the tribological and tribochemical interactions of different ferrous layers applied to nitride surfaces. *Journal of Tribology*, *143*(1), Article 011705. https://doi.org/10.1115/1.4047588

10. Liu, H. C., Zhang, B. B., Bader, N., Venner, C. H., & Poll, G. (2020). Simplified traction prediction for highly loaded rolling/sliding EHL contacts. *Tribology International*, *148*, Article 106335. https://doi.org/10.1016/j.triboint.2020.106335

11. Morales-Espejel, G. E., & Félix-Quiñonez, A. (2021). Application of a rolling bearing life model with surface and subsurface survival to hybrid bearings in high-load and high-speed applications. *Tribology Online*, *16*(4), 216–222. https://doi.org/10.2474/trol.16.216

12. Šperka, P., Krupka, I., & Hartl, M. (2016). Lubricant flow in thin-film elastohydrodynamic contact under extreme conditions. *Friction*, *4*(4), 380–390. https://doi.org/10.1007/s40544-016-0134-6

13. Wolf, M., Šperka, P., & Fatemi, A. (2022). Film thickness in elastohydrodynamically lubricated slender elliptic contacts: Part II – Experimental validation and minimum film thickness. *Proceedings of the Institution of Mechanical Engineers, Part J: Journal of Engineering Tribology*, *236*(12), 2361–2372. https://doi.org/10.1177/13506501221080289

Міланенко О., Богданов І., Леусенко Д., Вансовський О. Особливості мастильної дії олив в умовах ЕГД змащування в локальній зоні контакту тертя

На базі створеного стенду інтерференційних досліджень щодо оцінки товщини мастильного шару, що дозволяє реєструвати та аналізувати з високою точністю швидкоплинні процеси в умовах ЕГД змащування в зоні локального контакту тертя неконформних вузлів зі зміненою геометрією фактичної форми контакту, в широкому діапазоні робочих (кінематичних та навантажувальних) параметрів, було зроблено оцінку впливу швидкості, контактного навантаження, матеріалів пар тертя, реологічних властивостей мастильного матеріалу, геометрії форми контакту на процесс формування мінімальної і центральної товщини мастильного шару та режим мастильної дії олив в рамках визначення параметру мастильного шару.

Ключові слова: мастильна дія олив, еластогідродинамічне (ЕГД) змащування, інтерференційний випробувальний стенд, товщина мастильного шару, локальна зона контакту тертя, неконформні вузли, геометрія контакту, фактична форма контакту, реологічні властивості, еліптичний контакт, точковий контакт, параметр еліптичності.